COVER SHEET

Title: *Experimental Evaluation of Axial Crush Behavior of Woven Tubular Laminates with a Moving Support Condition*

Authors: Rudy T. Haluza
J. Michael Pereira
Charles R. Ruggeri
Justin D. Littell
Charles E. Bakis
Kevin L. Koudela

ABSTRACT

The objectives of the investigation were to measure the specific energy absorption (SEA) of the plain-weave carbon fiber reinforced polymer (CFRP) tubes, study the effect of tube length on SEA and stable crushing force, analyze the effect of using a crush trigger, and compare force-displacement data using different specimen support conditions. Dynamic crush testing of CFRP tubes was performed using the crash sled in the Impact Dynamics Laboratory at NASA Glenn Research Center. The sled features a movable mass that supports the specimen during crash testing. Laminated $[\pm 45]_4$ tubes were fabricated and tested using tube lengths of 102 mm or 152 mm each with a diameter of 76 mm. Sled impact velocities ranged from 6.15–6.48 m/s. In most tests, a crush trigger was applied to the front face of the tubes to initiate a crushing failure mode.

The mean SEA of the tubes tested with the crash sled was 48.6 J/g. There were virtually indistinguishable changes in failure modes for the 102-mm and 152-mm tubes. Plots of acceleration and cumulative absorbed energy for both tube lengths were nearly identical, which suggests that the effect of tube length on crush behavior was negligible in the range of tested impact velocities.

One of the 102-mm tubes was tested without a crush trigger to provide a direct comparison with a drop tower specimen that lacked a crush trigger. A higher peak force and lower SEA was measured for this specimen compared to the specimens that had a crush trigger. Both the peak force and stable crushing force were comparable for the drop tower and crash sled specimens lacking a crush trigger. However, the maximum crush displacement of the crash sled specimen was lower because a portion of the energy was absorbed by the motion of the support mass.

Rudy T. Haluza, Penn State University, University Park, PA 16802, USA
J. Michael Pereira, NASA Glenn Research Center, Cleveland, OH 44135, USA
Charles R. Ruggeri, NASA Glenn Research Center, Cleveland, OH 44135, USA
Justin D. Littell, NASA Langley Research Center, Hampton, VA 23681, USA
Charles E. Bakis, Penn State University, University Park, PA 16802, USA
Kevin L. Koudela, PSU Applied Research Laboratory, University Park, PA 16802, USA

INTRODUCTION

Project Background & Motivation

Littell et al. [1] investigated characteristics of a plain weave carbon fiber reinforced polymer (CFRP) tube specimen subjected to axial crush loading using a drop tower at NASA Langley Research Center. The CFRP featured in that study consisted of a plain-weave preform and epoxy applied using wet layup. This material was chosen because of its rapid fabricability and cost-effectiveness. The geometry was based on part of a prototype landing gear design for an urban air mobility vehicle concept. However, only acceleration data and maximum crush displacement were reported by Littell et al. [1].

To further experimentally characterize the axial crush response of the CFRP tube specimens, a horizontal crash sled in the Impact Dynamics Lab at the NASA Glenn Research Center [2] was used to further evaluate the axial crush response of the tubes and to compare the response of the $[\pm 45]_4$ tubes tested with the horizontal crash sled and a vertical drop tower. Specific (mass normalized) energy absorption (SEA), peak force, stable crushing force, and length effects were investigated using the sled.

The horizontal crash sled inherently differs from the vertical drop tower because the force of gravity can be ignored for all calculations involving the crash sled data. Therefore, when the specimen is impacted, there is no external force (except resistive forces that are often of low magnitude and thus neglected—e.g., friction and air resistance) acting on the impactor. In terms of instrumentation, the crash sled features force sensors, photogrammetry, and multiple accelerometers to provide independent measurements of the impact event [2]. In addition, the crash sled features a movable support mass that further differentiates the sled from typical crush testing methods.

Literature Survey

For optimum crashworthiness performance of composite structures, progressive crushing is desired [3]. Progressive crushing is defined by a relatively stable region in the force-displacement plot following an initial peak as depicted in Figure 1 [4]. Local peaks and valleys can be found in the progressive crushing zone due to the repeated collapse of structural sub-elements and transference of load to subsequent sub-elements [5]. This mechanism differs from a folding/buckling failure mechanism that has higher-magnitude undulations in the region between initial peak and unloading [6]. However, progressive crushing tends to lead to a higher SEA compared to folding/buckling [6]. Absorbed energy is calculated by integrating force as a function of displacement (i.e. computing the area under the force-displacement curve). SEA is calculated by dividing the energy absorbed by the mass of the crushed region of the specimen.

To further maximize the ability of a specimen to absorb energy, crush triggers are typically used to initiate a crushing failure mode [6] [7] [8]. Crush triggers are stress concentrators, fashioned on the end of a composite specimen that first contacts the impactor to initiate failure in this region. While geometries of crush triggers vary, bevel triggers, which involve chamfering of one edge, have been shown to be effective [6] [8]. The inclusion of crush triggers also lowers the initial peak force [9].

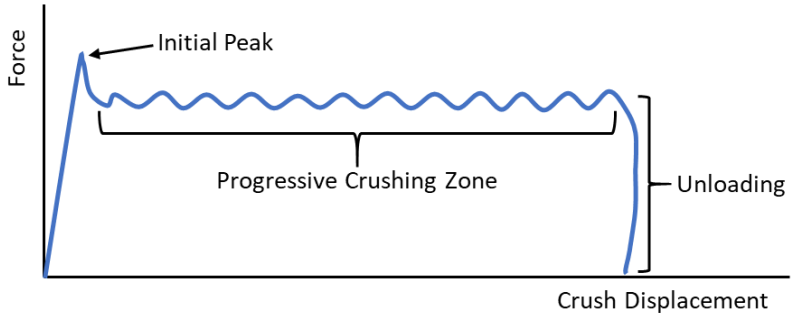

Figure 1. Characteristic plot of force versus crush displacement (force-displacement curve) for a composite specimen undergoing progressive crushing with labeled regions.

Farley [10] showed that SEA is dependent on the specimen geometry, fibers, fiber layup, and matrix comprising the composite structure. Farley [10] also showed that, in terms of SEA, there is a local maximum for tube laminates with [±θ] layups at 45°. In addition, Farley [10] reported a SEA value of 38.5 J/g for a $[\pm 45°]_n$ CFRP cylindrical tube with a diameter to thickness ratio of 60, which are comparable to the tubes in the present investigation.

PROCEDURES

Crash Sled Testing

Dynamic crush testing was performed using the crash sled in the Impact Dynamics Laboratory at NASA Glenn Research Center. The crash sled and data acquisition instrumentation are illustrated in Figure 2. The specimen is attached to a support mass (M_2), which is initially at rest but free to move in the axial direction. The impactor mass of the sled (M_1) is propelled into the specimen by a pneumatically actuated ram. The ram separates from M_1 just prior to impact. Force sensors behind the specimen plate, accelerometers on both masses, and photogrammetry are used to record the impact event, as described in Table I. Photogrammetry directly measures the displacement.

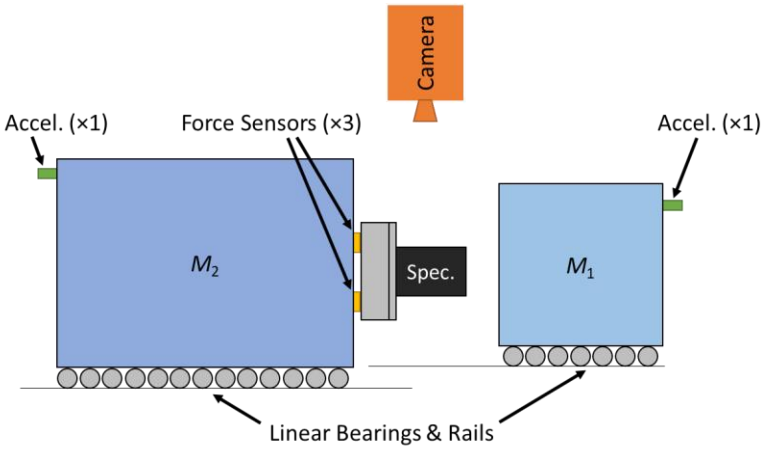

Figure 2. NASA Glenn Ballistic Impact Lab crash sled setup with impactor mass (M_1), stopper mass (M_2), specimen, force sensors, specimen plate (M_{PL}), camera, and accelerometers (not to scale).

TABLE I. INSTRUMENTATION FOR DATA ACQUISITION

Equipment	Make & Model	Record Rate	Range
Force Sensor (×3)	PCB[a] 203B/FCS-5	1.25 MHz	89 kN
M_1 Accelerometer	PCB[a] ICP 350C04	1.25 MHz	5000 g
M_2 Accelerometer	Kistler[b] 8704B5000	1.25 MHz	5000 g
High-speed Camera	Photron[c] Fastcam SA-Z	70000 fps	N/A

[a]PCB Piezotronics (Depew, New York), [b]Kistler Group (Winterthur, Switzerland), [c]Photron (Tokyo, Japan)

A picture of the sled is shown in Figure 3. For this investigation, M_1 was 40.01 kg, M_2 was 319.66 kg, and M_{PL} was 6.3 kg. More information about the crash sled setup, mechanics, and data processing methodology is provided by Ruggeri et al. [2].

Due to available material, the mass of the impactor for the crash sled was 13.5% lower than the drop tower impactor. To emulate the testing performed by Littell et al. [1], a nominal impact velocity of 6.4 m/s was selected to equalize the kinetic energy of the crash sled impactor and the drop tower impactor. Because pneumatic actuation of M_1 leads to variability in velocities, M_1 velocities ranged between 6.15–6.48 m/s.

CFRP Tubes

The CFRP tubes consisted of a $[\pm 45]_4$ laminate manufactured at the NASA Langley Research Center by wet-layup. The fabric consists of TR 30S carbon fibers (Mitsubishi Chemical Carbon Fiber and Composites, Sacramento, CA) woven in a balanced plain weave pattern with a fiber areal weight of 193 g/m^2. A single rectangular piece of fabric was cut at a 45° angle to the warp direction, impregnated by hand with West System 105/205 epoxy (West System, Bay City, MI, USA), and hand wrapped with four complete revolutions around a 76-mm-diameter removable mandrel to fabricate the tubes. The as-wrapped tubes were cured overnight at room temperature, and the mandrel was extracted afterward. Based on the fiber areal weight, a measured cured ply thickness of 0.25 mm, and an assumed fiber mass density of 1.79 g/cm^3, a fiber volume fraction of 0.43 was calculated. The tubes had a nominal thickness of 1.0 mm. The CFRP tubes were manufactured at a nominal length of 254 mm and were cut to the desired 152-mm length (Figure 4a). However, the remaining 102-mm-long tubes (Figure 4b) were also tested as separate specimens. More information regarding specimen manufacturing is available in Littell et al. [1].

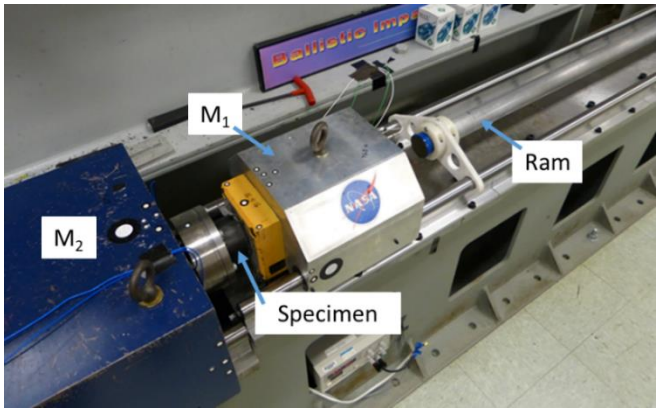

Figure 3. Photograph of crash sled and specimen after a completed test (with labeled parts). Note that the front (yellow) plate on M_1 is 51 mm in length (direction of rails) for scale.

(a) (b)

Figure 4. CFRP plain-weave 152-mm tube specimen (a) and 102-mm tube specimen (b). The crush trigger is labeled on each specimen with an "I" and the specimen ID (PA##) on the opposite end.

To produce the crush trigger, a router was placed in a vice, and the tube was manually rotated at a 45° relative to the rotational axis of the router-head, thus applying the bevel trigger to the inner diameter of the front edge of the tube. Figure 5 shows the inner diameter of a tube with a crush trigger.

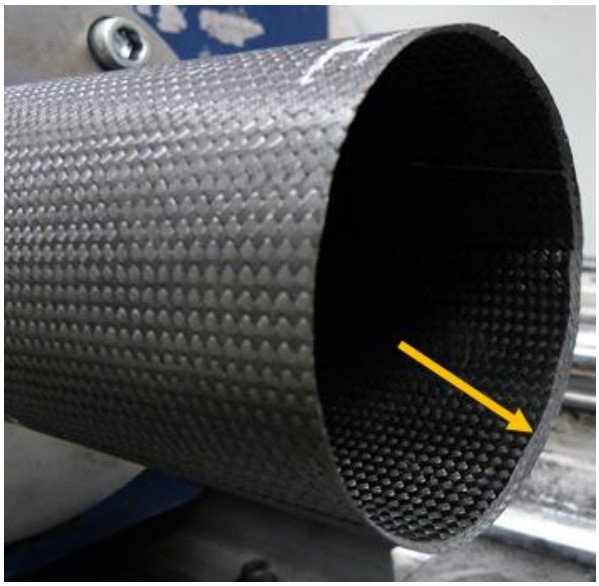

Figure 5. Example of a crush trigger routed into the end of a 76-mm diameter tube specimen.

Table II lists the number of specimens tested for each specimen length (e.g. 102-mm and 152-mm). One of the 102-mm specimens was tested without a crush trigger to compare the response of specimens with the crush trigger to a specimen without a trigger and to directly compare a sled specimen to the CFRP tube tested using the drop tower, which did not have a crush trigger.

TABLE II. TEST MATRIX FOR CRASH SLED TESTING

	102-mm	152-mm
Number of Specimens	4*	4

*One of the four 102-mm specimens was tested without a crush trigger

Comparison to Drop Tower Data

To compare impact forces measured by the crash sled instrumentation and drop tower accelerometer, it was necessary to incorporate the acceleration of gravity before converting accelerometer measurements to forces via Newton's second law. This process is shown in Equations 1 and 2, and the free-body diagram that accompanies Equation 1 is shown in Figure 6, where m and a denote the mass and acceleration of the drop tower impactor, F_g is the gravitational force, F_{imp} is the impact force (i.e. the reaction force of the specimen during impact), and g is the gravitational constant [11].

$$\Sigma F = ma = F_{imp} - F_g \quad (1)$$

$$F_{imp} = ma + F_g = m(a + g) \quad (2)$$

Figure 6. Free body diagram of drop tower impactor. Equations 1 and 2 demonstrate the necessity for adding a correction factor before calculating impact force for drop tower.

Because the drop tower only has an accelerometer on the impactor, displacement is not directly measured. Thus, displacement data were computed from the acceleration data by performing two integrations using the trapezoidal rule. The constant of integration for velocity was chosen to make the maximum velocity before impact equal to 5.97 m/s, equivalent to the speed reported by Littell et al. [1]. The constant of integration for displacement was selected to align the peak force of the plots.

RESULTS

CFRP Tubes with Crush Triggers

The 102-mm and 152-mm CFRP tubes in each test did not fully crush (bottom out), which suggests all tests were valid. A sequence of images from the photogrammetry of one of the 152-mm tubes is shown in Figure 7 that spans from the time of impact to separation of M_1 and the crushed specimen. In Figure 7, the impacting mass is moving from left to right.

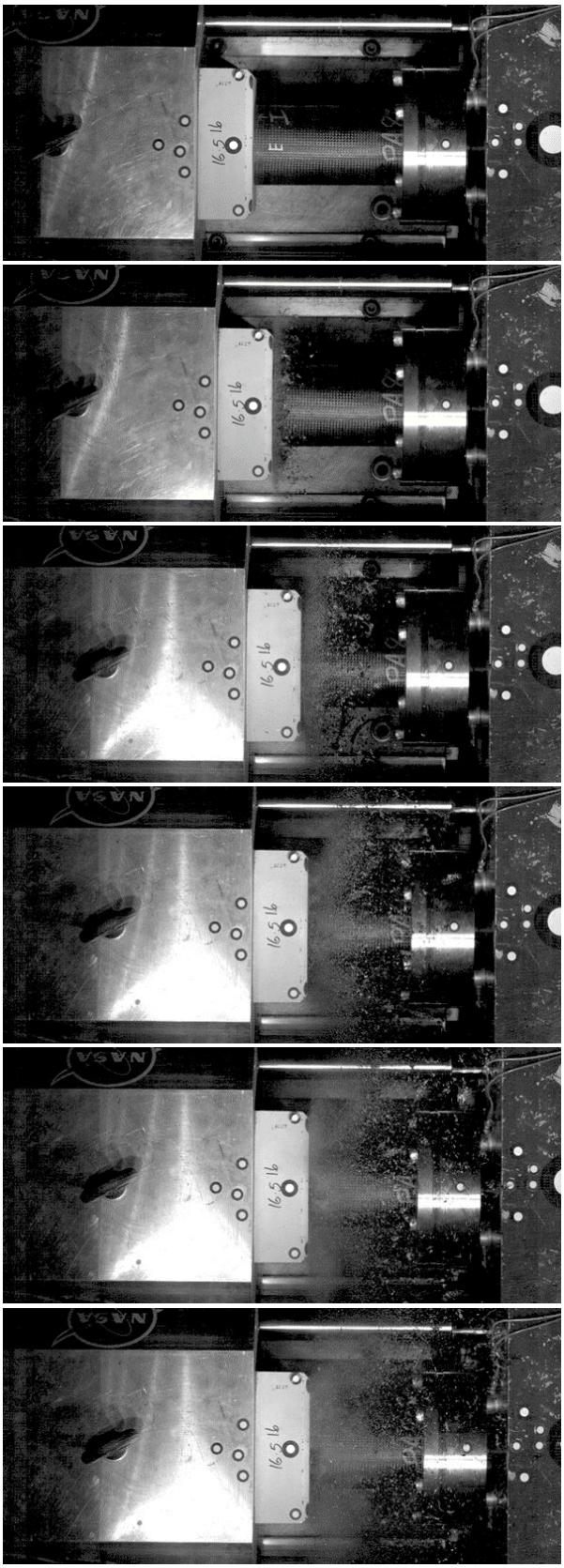

Figure 7. Sequenced grayscale images from photogrammetry showing crushing of a 152-mm specimen. Intervals are spaced by 0.0071 s and begin from approximately the time of impact and end after the specimen has separated from M_1. Note the 76-mm diameter of the tube for scale.

As shown in Figure 8 and Figure 9, the 102-mm and 152-mm tubes failed in a similar manner, which was a combination of transverse shearing and lamina bending [12]. Fronds formed because of matrix delamination at the interface of the [±45] layers. The virtually indistinguishable failure modes indicate that the tube length at impact velocities of 6.5 m/s has a negligible effect on the failure response.

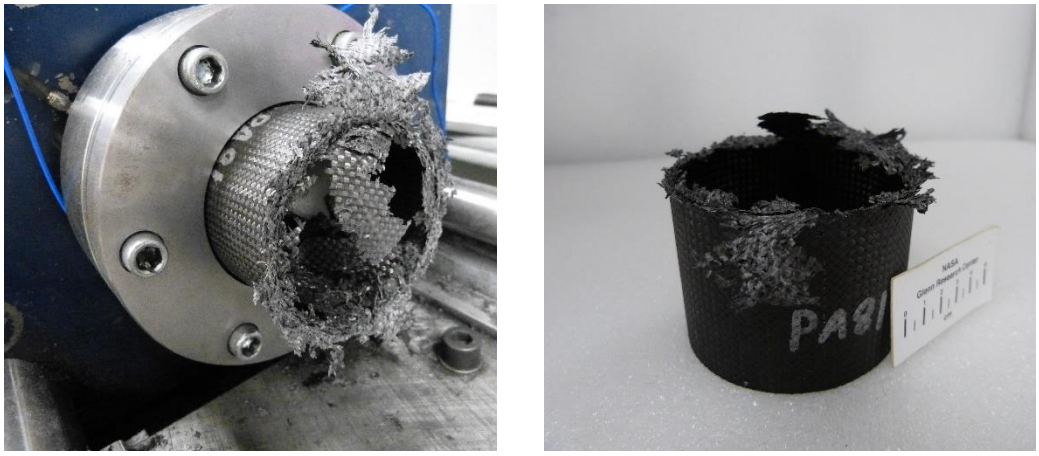

(a) (b)

Figure 8. Post-impact pictures of a 102-mm tube a) bolted to the sled and b) removed from the sled.

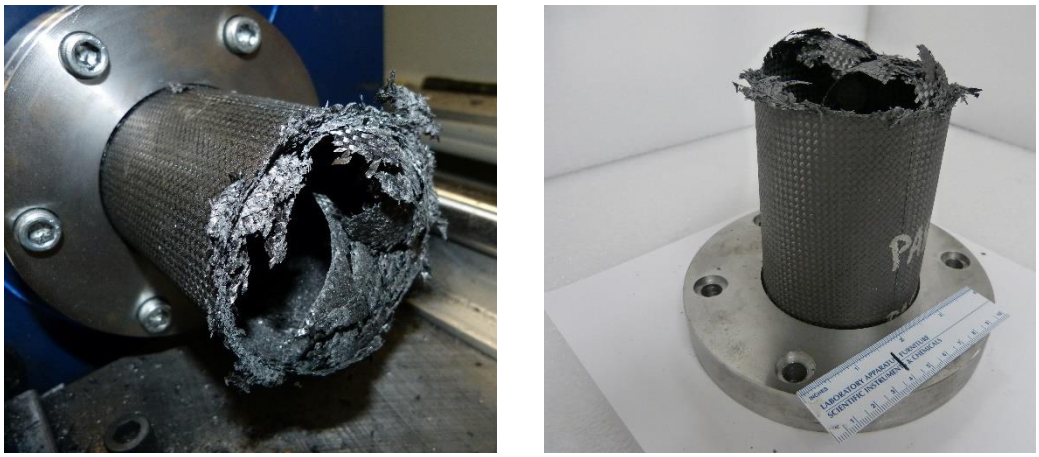

(a) (b)

Figure 9. Post-impact pictures of a 152-mm tube a) bolted to the sled and b) removed from the sled.

The indiscernible effects of tube length failure modes are further supported by the SEA values summarized in Figure 10, which shows a comparison of the SEAs measured for each specimen length using the four methods of measuring SEA using the crash sled instrumentation. While the measured SEAs of the 152-mm tubes are slightly higher than those of the 102-mm tubes, the difference falls within the experimental scatter. The difference between the highest- and lowest-measured SEA for each specimen length is approximately 5%. This relatively small difference provides confidence in the measured SEA values, which is approximately 48.5 J/g if each of the eight SEAs reported in Figure 10 are averaged.

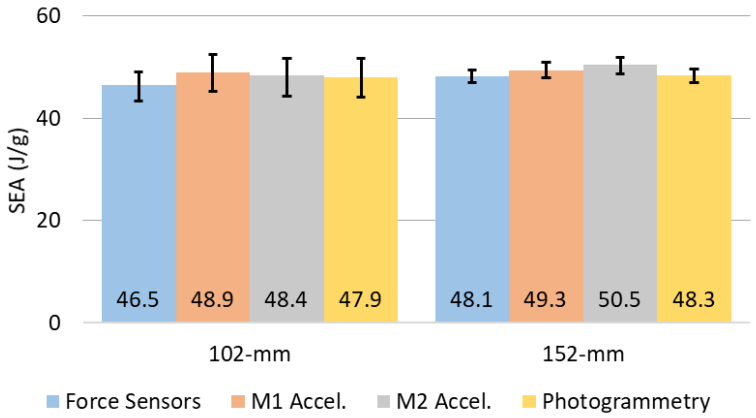

Figure 10. Comparison of mean SEA values from four sensors for 102-mm tubes (3 specimens), 152-mm tubes (4 specimens). Error bars depict the highest- and lowest-measured SEAs. All specimens included in this dataset had crush triggers.

The relatively minor difference in the crush response of the 102-mm tubes and 152-mm tubes can also be seen in the force-displacement. A comparison of two representative specimens from each specimen length is shown in Figure 11.

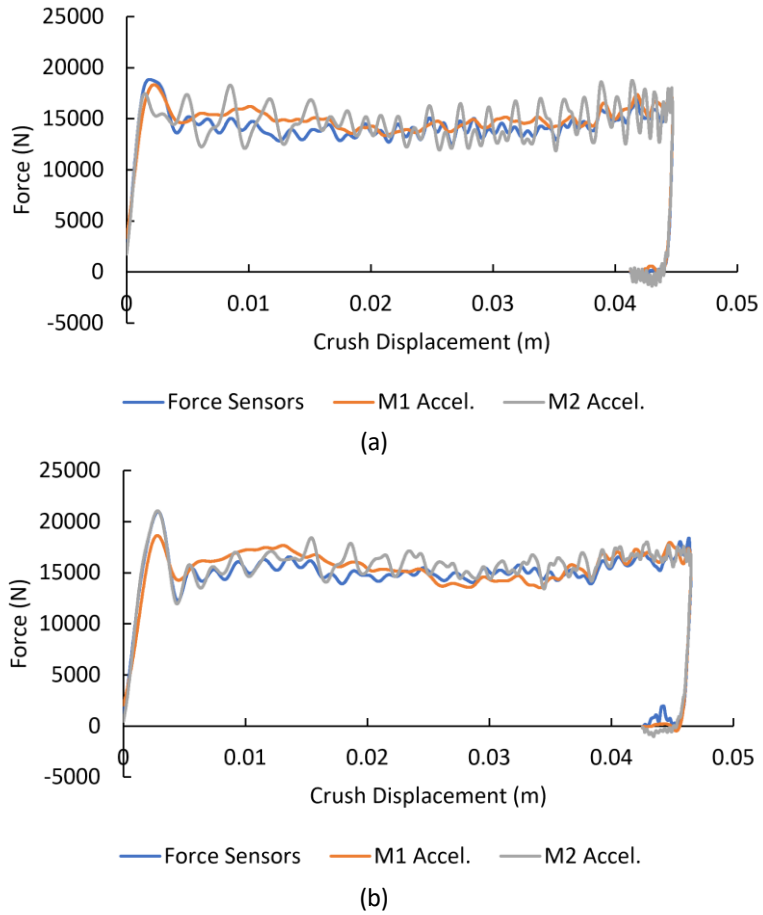

Figure 11. Force-displacement plots for (a) a 102-mm tube and (b) a 152-mm tube representative of their respective specimen length. Data were filtered using a 200 Hz cutoff low-pass Butterworth filter.

Although the tube specimens vary in length, both the 102-mm and 152-mm tubes exhibit approximately the same stable crushing force (i.e. the force in the region between initial peak and unloading) and maximum crush displacement. The filtered data plotted in the force-displacement curves for the crash sled specimens does not start at zero force due to the time shift that occurs during filtering; thus, while the unfiltered forces are zero when crush displacement is zero, the filtered curves are slightly higher than zero.

To further show the similarity in the response of the 102-mm and 152-mm tubes tested with the crash sled, the cumulative energy absorbed versus crush displacement data are plotted together in Figure 12. This plot depicts the area under the force-displacement curves, and the slope is directly proportional to the SEA. The overlapping nature of these curves suggests that the response from the 152-mm and 102-mm tubes are practically indistinguishable.

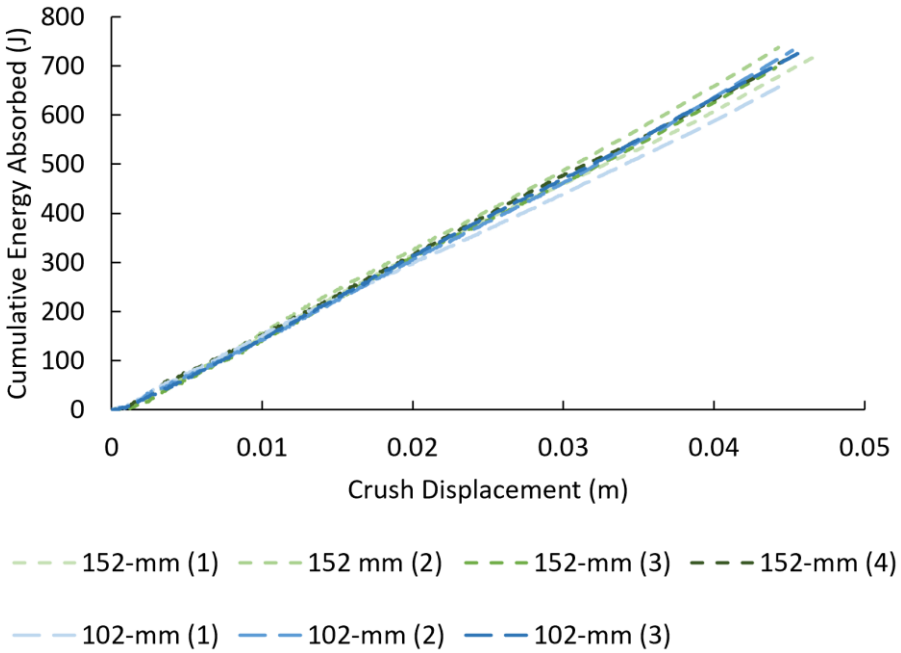

Figure 12. Cumulative energy absorbed versus displacement plots for all tubes with a crush trigger. Based on data measured by the M_1 accelerometer. Dashed lines used for clarity because lines overlap.

In addition to the photogrammetry data already presented, a thermal camera was set up next to the specimen as an exploratory study on measuring changes in temperature during crash sled testing. The camera had a recording rate of 220 frames per second. Thermal images at several points during the impact event are displayed in Figure 13. The emissivity of the 152-mm composite tube specimen was not calculated or input into the camera settings prior to testing, so the absolute temperature values reported by the thermal camera are not necessarily correct. However, there are significant changes in the surface temperature of the composite tube specimen during the impact event. These preliminary thermal results suggest that future investigations of the change in temperature of composite specimens undergoing dynamic crush impact could benefit our understanding of failure and energy absorption mechanisms.

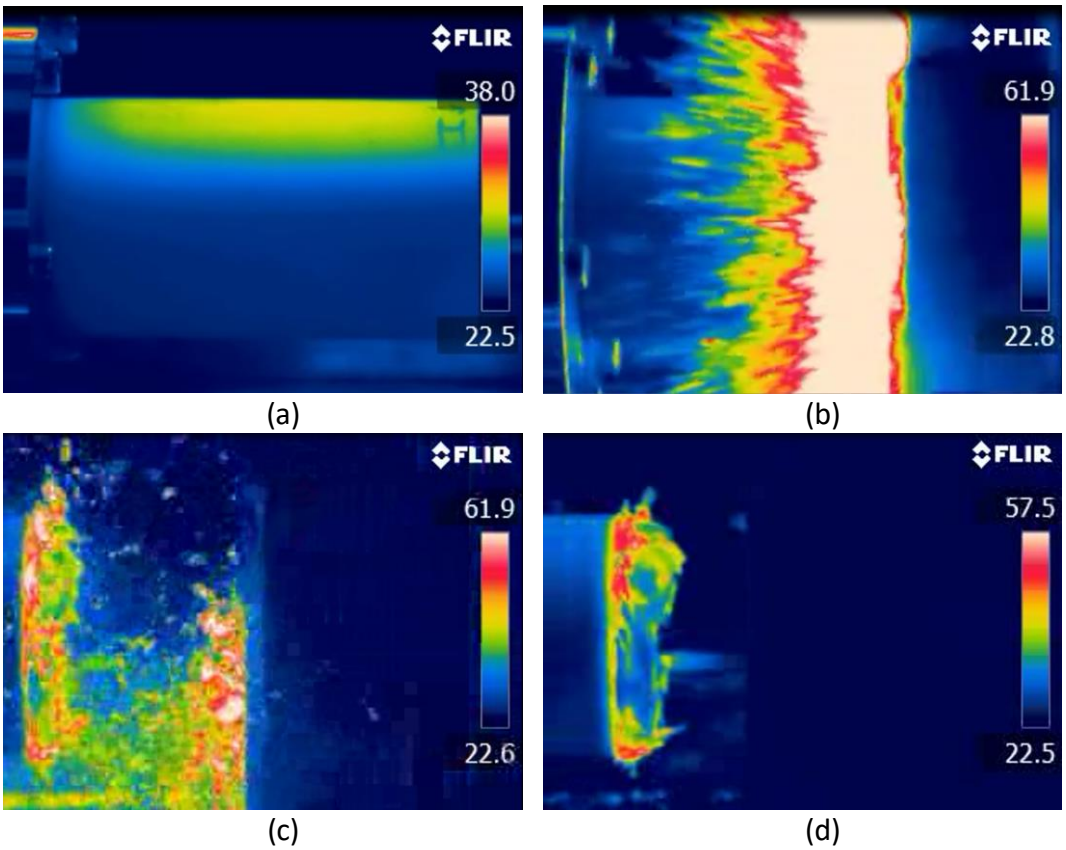

Figure 13. Thermal imaging of a 152-mm tube at several points during the impact event including a) before impact—specimen attached to M_2 on left-side; to be impacted by M_1 on right-side (note that lighting for top-view photogrammetry leads to uneven heating prior to impact), b) at first contact with the impacting mass, c) the last frame before the specimen leaves the frame of view, and d) when the specimen first re-enters the camera view after M_2 has rebounded off the spring at the end of its rails. Note that the scale is in degrees Celsius, however, the emissivity of the specimen was not calculated or input into the camera settings prior to testing.

Specimen without Crush Trigger

One additional specimen was tested without a crush trigger. The force-displacement curve of this specimen is shown in Figure 14. Compared to the specimens that have a crush trigger, the specimen without a crush trigger demonstrates a higher initial peak force followed by a drop to near-zero force and a return to the stable crush force thereafter, which is similar in value to the specimens with the trigger. Due to this region, the average SEA (37.3 J/g) for this specimen was 23% lower than specimens that had the trigger. Lower SEAs are commonly measured in specimens without crush triggers [4].

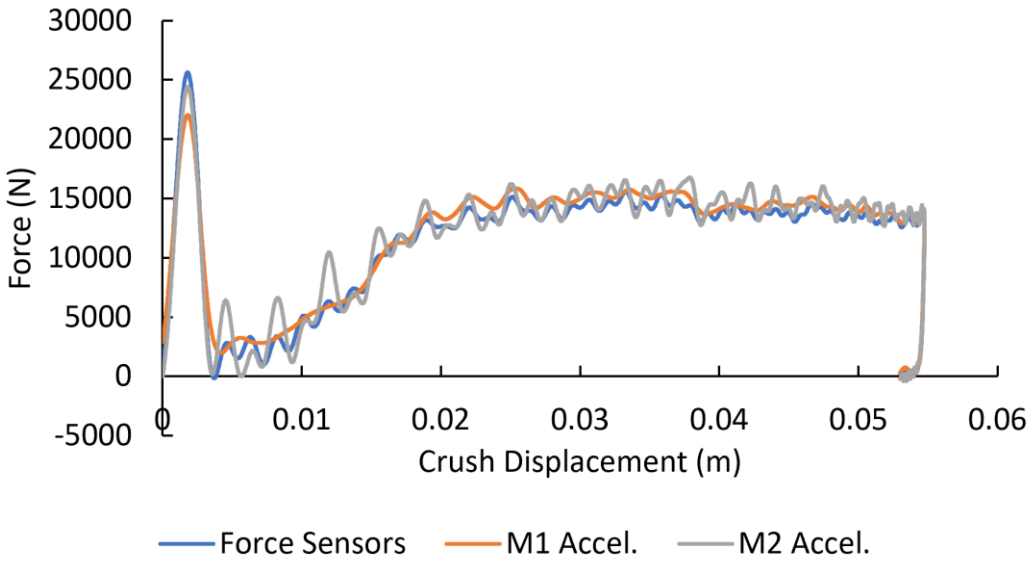

Figure 14. Force-displacement curve for a 102-mm tube without a crush trigger. Data were filtered using a 200 Hz cutoff low-pass Butterworth filter.

Comparison to Drop Tower Data

The force-displacement curve for the crash sled specimen without a crush trigger was compared to a drop tower specimen (also lacking a trigger) as shown in Figure 15. Note that displacement was not directly measured in the drop tower setup, so a dashed line was used to plot the calculated drop tower force-displacement result.

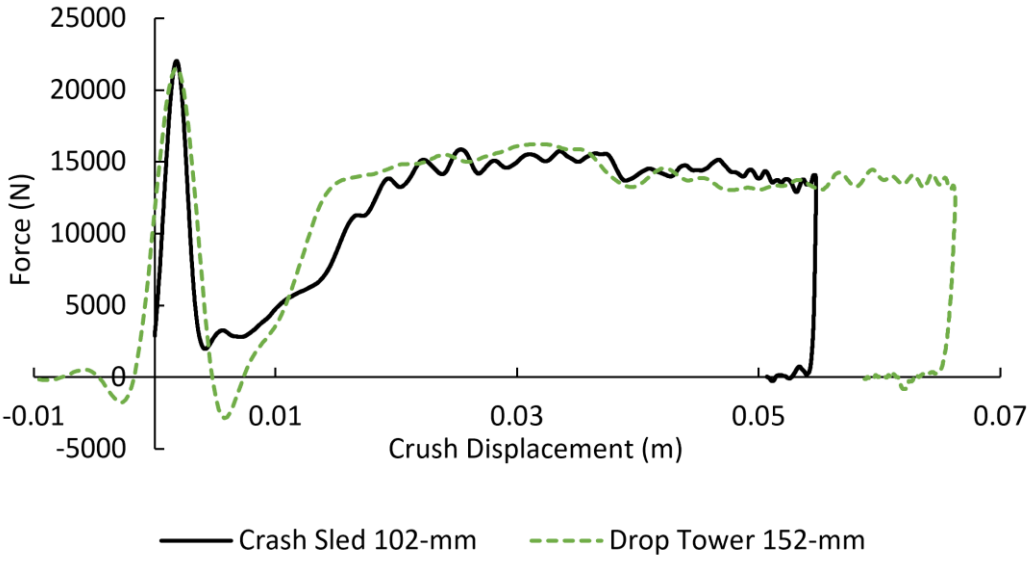

Figure 15. Comparison of force-displacement curves from tubes tested with the crash sled and drop tower. Note a dashed plot was chosen for the drop tower specimen to signify that crush displacement was computed from acceleration data as opposed to direct measurement with the crash sled specimen. Data for crash sled specimen is from the accelerometer on M_1 and was filtered using a 200 Hz cutoff low-pass Butterworth filter.

Littell et al. [1] reported a maximum crush displacement of 66 mm, and the same value was derived from the acceleration data and plotted in Figure 15. The maximum displacement for the crash sled specimen without a crush trigger was 54.8 mm. To further compare, specimens that had a crush trigger and were tested using the crash sled had a mean maximum crush displacement of 45.0 mm. The lower crush displacement of the crash sled specimens is due to the non-fixed boundary (M_2), which allows some of the impact energy to be absorbed through the motion of the support mass. However, the peak force and stable crushing force are essentially the same for both specimens.

The drop tower specimen differs from the crash sled specimen in the region between the peak and progressive crushing zone. In this region, the drop tower impactor force dips below zero before sharply reversing direction and stabilizing. This notable difference may be due to the different boundary conditions of the two systems. The non-fixed boundary of the crash sled allows for a gentler transition into the stable region than the fixed boundary of the drop tower.

CONCLUSIONS & FUTURE WORK

Conclusions

An investigation characterizing the crush response of CFRP tube specimens, manufactured using a woven architecture and wet layup, was conducted using a crash sled designed at NASA Glenn Research Center. The tube specimens were of interest due to their rapid manufacturability and cost-effectiveness for future urban air mobility vehicles. The crash sled features a movable support mass as well as force sensors, accelerometers, and photogrammetry that enable multiple independent measurements of the impact event.

Four major results were observed. The crush response of the 102-mm and 152-mm tubes with crush triggers tested with the crash sled were practically identical in terms of the force-displacement curve, specific energy absorption (SEA), and the observed failure mechanism. The SEA of the tube specimens was found to be 48.5 J/g. Removing the crush trigger from the specimens increased the peak force and produced a region of unloading and reloading between the peak force and stable region, thus lowering the SEA, which has been observed by other researchers [4]. Finally, specimens without triggers tested with the drop tower and crash sled were compared. The peak force and stable crushing force were similar; however, the drop tower specimen had a higher maximum crush displacement and a different shape in the region of unloading and reloading between the peak force and stable region. Both of these observations are likely a result of the different boundary conditions for the drop tower and crash sled.

Future Work

There are several opportunities for future investigation based on the findings of this test program. Specimens with crush triggers can be tested using the drop tower to further compare the two methods of measuring the crush response of CFRP tubes. Similarly, carbon/aramid hybrid tubes tested using the drop tower could be compared to hybrid tubes tested using the crash sled. However, a folding failure mode is common when crushing tubes with aramid fiber reinforcement due to the high strain-to-failure of the

aramid fibers [3]. Thus, it may be necessary to change one or more parameters of the hybrid tubes (e.g. specimen dimensions, trigger geometry, etc.) to initiate progressive crushing.

While the results from the thermal camera in this study were inconclusive, there is an opportunity for measuring changes in temperature during crash sled testing. Temperature changes are important for two reasons. Researchers have shown that SEA decreases in CFRPs with epoxy matrices at higher temperatures, especially temperatures exceeding 150°C [7]. In addition, because friction plays a major role in energy absorption in crush testing [12], change in temperature may aid in quantifying the energy absorbed due to friction inside the CFRP during crushing and friction between the impactor and specimen.

REFERENCES

1. Littell, J., J. Putnam, and R. Hardy. 2019. "The Evaluation of Composite Energy Absorbers for Use in UAM EVTOL Vehicle Impact Attenuation," in *Proc. AHS Forum 75, Vertical Flight Society*, Philadelphia, PA, USA, 15 p.
2. Ruggeri, C. R., R. T. Haluza, J. M. Pereira, S. G. Miller, C. E. Bakis, and K. L. Koudela. 2021. "Crash Sled Testing of Triaxially-Braided CFRP for Improved Vehicular Crashworthiness," accepted for publication in *Proc. ASCE Earth and Space Conference 2021*, Seattle, WA, USA.
3. Jacob, G. C., J. F. Fellers, S. Simunovic, and J. M. Starbuck. 2002. "Energy Absorption in Polymer Composites for Automotive Crashworthiness," *J. Compos. Mater.*, *36*(7), 813-850.
4. Garner, D. M. and D. O. Adams. 2008. "Test Methods for Composites Crashworthiness: A Review," *J. Adv. Mater.*, *40*(4), 5-26.
5. Czaplicki, M. J., R.E. Robertson, and P. H. Thornton. 1991. Comparison of Bevel and Tulip Triggered Pultruded Tubes for Energy Absorption. *Compos. Sci. and Tech.*, *40*(1), 31-46.
6. Hull, D. 1991. "A Unified Approach to Progressive Crushing of Fibre-Reinforced Composite Tubes," *Compos. Sci. and Tech.*, 40(4), 377-421.
7. Thornton, P. H., J. J. Harwood, and P. Beardmore. 1985. "Fiber-Reinforced Plastic Composites for Energy Absorption Purposes," *Compos. Sci. and Tech.*, 24(4), 275-298.
8. Jimenez, M. A., A. Miravete, E. Larrode, and D. Revuelta. 2000. "Effect of Trigger Geometry on Energy Absorption in Composite Profiles," *Compos. Struct.*, 48(1-3), 107-111.
9. Thuis, H. G. S. J. and V. H. Metz. 1994. "The Influence of Trigger Configurations and Laminate Lay-Up on the Failure Mode of Composite Crush Cylinders," *Compos. Struct.*, 28(2), 131-137.
10. Farley, G. L. 1989. "Energy-Absorption Capability of Composite Tubes and Beams". Doctoral Dissertation, Virginia Polytechnic Institute and State University.
11. Browne, A. L., and Johnson, N. L. 2002. "Dynamic crush tests using a 'free-flight' drop tower: theory," *Experimental Techniques*, *26*(5), 43-46.
12. Farley, G. L., and R. M. Jones. 1992. "Crushing Characteristics of Continuous Fiber-Reinforced Composite Tubes," *J. of Compos. Mater.*, *26*(1), 37-50.